High Resolution Optical Spectroscopy of *mer*-[Cr(dpt)(Gly-Gly)]ClO4

Jong-Ha Choi

Department of Chemistry, Andong National University, Andong 760-749, Korea
Received January 14, 1999

The highly resolved absorption spectra of *mer*-[Cr(dpt)(Gly-Gly)]ClO4·H2O [dpt = di(3-aminopropyl)amine, H2Gly-Gly = glycylglycine] have been measured between 13000 cm^{-1} and 50000 cm^{-1} temperatures down to 2 K. The vibrational intervals were extracted by recording emission and far-infrared spectra. The characteristic infrared bands in meridional isomer were discussed. The fourteen electronic origins due to spin-allowed and spin-forbidden transitions were assigned. With the use of this electronic transitions, a ligand field optimization based on the exact known ligand geometry have been performed to determine more detailed bonding properties of Gly-Gly and dpt ligands. It is confirmed that the peptide nitrogen of the Gly-Gly has a weak π-donor property toward chromium(III) ion.

Introduction

A few investigations have been made on the spectroscopic and structural properties of chromium(III) complexes with the dipeptides series.[1~4] In these complexes with dipeptides as tridentate ligand, the three donor atoms (carboxylate-O, amido-N and amino-N) of a dipeptides ligand are located in meridional disposition. Dipeptides such as glycylglycine generally form meridionally coordinated complexes as tridentate ligand because the coordinating peptide nitrogen atom is constrained to approximate coplanarity. Thus they can act as strong template ligands to synthesize meridionally coordinated complexes with other tridentate ligands. Di(3-aminopropyl)amine (dpt) has a moderate preference for meridional coordination, though facial coordination has been found in at least one mononuclear compound.[5,6]

Recently a considerable amount of data concerning sharp-line electronic spectroscopy of chromium(III) complexes has been accumulated.[7~16] It has been recognized that the intraconfiguration *d-d* transitions may be useful to determine metal-ligand bonding property as well as molecular geometry. Especially the sharp-line splittings are very sensitive to the exact bond angles around the metal. Thus it is possible to extract structural information from sharp-line electronic spectroscopy without a full X-ray structure determination.[17,18]

In this study the low temperature absorption and emission spectra, and the room temperature infrared spectra of *mer*-[Cr(dpt)(Gly-Gly)]ClO4·H2O have been measured. The pure electronic origins were assigned by analyzing the vibrational and absorption spectra. Using the observed electronic transitions, a ligand field analysis have been performed to determine the metal-ligand bonding properties for the coordinated atoms toward chromium(III) ion.

Experimental Section

Synthesis. The chemicals were of reagent grade or better quality and used without further purification. The complex *mer*-[Cr(dpt)(Gly-Gly)]ClO4·H2O was prepared as described previously.[3] The compound was recrystallized three times for spectroscopic measurements.

Physical Measurements. The low-temperature absorption spectra were measured on polyethylene matrix by using a Cary 5e spectrometer. The pellets were cooled to 2 K by a Cryvac helium cryostat. The emission spectra were obtained using an argon-ion laser (Spectra Physics 2045) pumped Ti:sapphire laser (Schwartz Electrooptics) in standing wave configuration. Wavelength control was achieved by an inch-worm driven (Burleigh PZ 501) birefringent filter. The sample emission was dispersed by a 0.85m double monochromator (Spex 1402) and detected by a cooled photomultiplier (RCA 31034) using a photoncounting system (Standard Research 400). Sample cooling for emission measurements at 10 K was achieved using the helium-gas flow technique.[19] The far-infrared spectra were recorded with a Bruker 113v instrument on a microcrystalline sample pressed in to a polyethylene pellet. The mid-infrared spectra were recorded with a Mattson 2020 Galaxy FT-IR spectrometer on a KBr disk. The 2 mg compound was pressed into 100 mg of polyethylene or KBr disks by using a Spex 3624B X-Press.

Results and Discussion

Infrared and Emission Spectra. The infrared spectroscopy is frequently useful in elucidating structures and determining the number of functional groups involved in coordination by a multidentate ligand. In some cases stretching and bending modes of amino groups in metal-amino acid complexes are sensitive to the stereochemistry of the complexes. Meridional coordinated ligands have different stretching, bending and rocking frequencies in the infrared region than facially coordinated ligands. Figure 1 presents the mid-infrared spectrum recorded at room-temperature of *mer*-[Cr(dpt)(Gly-Gly)]ClO4·H2O.

A sharp absorption peak at 3590 cm^{-1} can easily assigned to the O-H stretching of H2O molecule in the hydrate complex. The strong bands in the regions of 3100-3300 cm^{-1} and 2800-3000 cm^{-1} due to the symmetric and antisymmetric N-H and C-H stretching modes, respectively. Infrared spectra
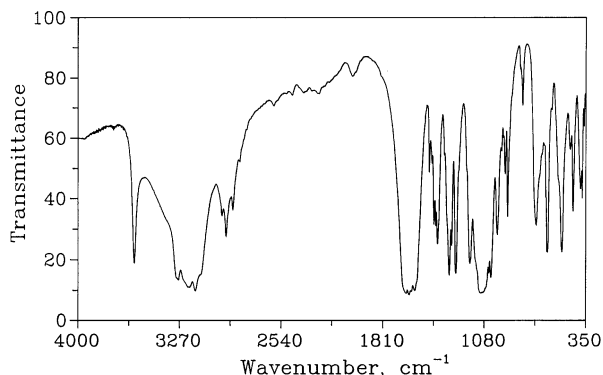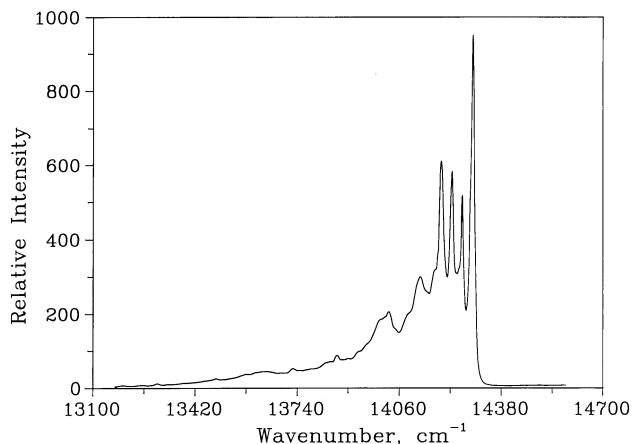
Figure 1. Mid-infrared spectrum of *mer*-[Cr(dpt)(Gly-Gly)]ClO₄·H₂O at 298 K.

can be used diagnostically to identify the meridional isomer of complexes with tridentate ligands which have coordinating atoms constrained to approximate coplanarity. The carboxylate stretching frequency of glycylglycinate is found at 1576 cm⁻¹ and amide carbonyl stretching frequency at 1624 cm⁻¹ indicating that both the carboxylate and the deprotonated amide nitrogen of glycylglycine are coordinated. As in [CoCl(dpt)(tn)]ZnCl₄, [Cr(dpt)(Gly-Gly)]ClO₄·H₂O also has four CH₂ rocking peaks in the 900-1000 cm⁻¹ region and several peaks in the 1500-1600 cm⁻¹ region.[20] Schmidtke and Garthoff's scheme for different isomers of dien can be used for the homologous dpt complexes because of the similarity in their basic structures.[21] As described in that scheme, the infrared spectrum of [Cr(dpt)(Gly-Gly)]ClO₄·H₂O has two NH₂ rocking peaks near 850 cm⁻¹ as 814 and 805 cm⁻¹. One band (712 cm⁻¹) between 700 and 800 cm⁻¹ is from the glycylglycinate ligand. The N-H wagging mode appears at 1288 cm⁻¹ as a medium band. The N-H stretching mode near 2850 cm⁻¹ for the secondary amine in dien is characteristic of meridional isomers. For the dpt, we can also expect the secondary amine N-H stretching mode near 2850 cm⁻¹. There is a corresponding medium intense peak at 2880 cm⁻¹ in *mer*-[CrCl₃(dpt)]. The result confirms that this band can be used to distinguish meridional from facial isomers. The medium intensity band at 2885 cm⁻¹ shows that this band is characteristic of meridional coordination.[22] The configuration of glycylglycinate in [Cr(dpt)(Gly-Gly)]ClO₄·H₂O was
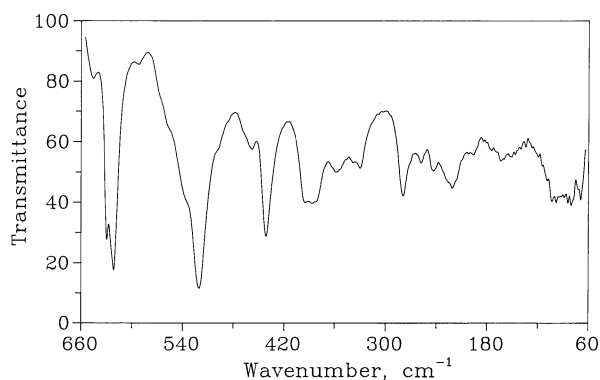
Figure 2. Far-infrared spectrum of *mer*-[Cr(dpt)(Gly-Gly)]ClO₄·H₂O at 298 K.

Figure 3. The 530 nm excited emission spectrum of *mer*-[Cr(dpt)(Gly-Gly)]ClO₄·H₂O at 10 K.

established as meridional geometry by our single crystal X-ray structure determination.[4] The far-infrared spectrum is also shown in Figure 2. The strong peaks at 441 and 470 cm⁻¹ can be assigned to the Cr-N$_a$ stretching mode.[23] A number of absorption bands in the range 285-50 cm⁻¹ arise from lattice vibrations and skeletal bending modes.

An experimental problem lies with the difficulty in distinguishing pure electronic components from the vibronic bands that also appear in the sharp-line spectrum. In addition to far-infrared spectrum, emission spectrum can be used to extract the vibrational intervals of electronic ground state. The 530 nm excited emission spectrum of *mer*-[Cr(dpt)(Gly-Gly)]ClO₄·H₂O at 10 K is shown in Figure 3. The band positions relative to the lowest zero phonon line, with corresponding infrared frequencies, are listed in Table 1.

The very strong peak at 14291 cm⁻¹ can be assigned to the zero-phonon line, R_1 because a corresponding strong peak is found at 14294 cm⁻¹ in the absorption spectrum. A well

Table 1. Vibrational frequencies from the 10 K emission and 298 K infrared spectra of *mer*-[Cr(dpt)(Gly-Gly)]ClO₄·H₂O[a]

Emission[b]	Infrared	Assignment
-208 w		R_2
0 vs		R_1
33 m		
66 s	69 vw	
100 vs	80 w, 98 w	Lattice vib.
167 m	170 w	and
	221 m	Skeletal bends
263 m	243 w	
290 w	280 s	
342 w	330 m, 358 m	ν (Cr-N$_p$)
	387 m	ν (Cr-O)
426 m	441 vs, 470 m	ν (Cr-N$_a$)
566 m	520 vs	
	621 s	ClO₄⁻
654 w	630 s	
711 vw	708 m	
808 w	805 w	ρ (NH₂)
909 w	913 m	

[a] Data in cm⁻¹. [b] Measured from zero-phonon line at 14291 cm⁻¹.

438 *Bull. Korean Chem. Soc.* **1999**, Vol. 20, No. 4

Jong-Ha Choi
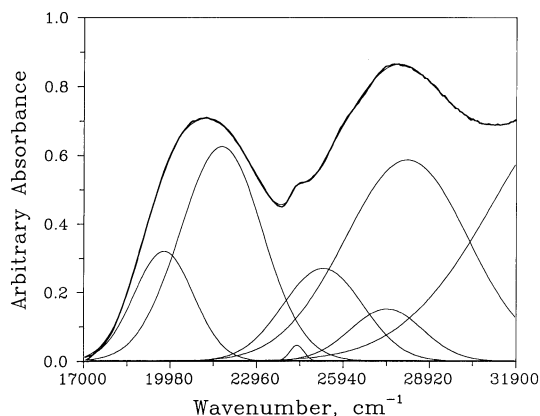
defined hot band at 14499 cm^{-1} may be assigned to the second component, R_2 of the $^2E_g \rightarrow ^4A_{2g}$ transition. The vibrational intervals occurring in the spectrum consist of several modes can be presumed to involve primarily ring torsion and angle-bending modes with frequencies below 285 cm^{-1}. The Cr-N$_a$ stretching mode can be assigned to the 426 cm^{-1} vibronic band.

Absorption Spectra. The visible absorption spectrum of *mer*-[Cr(dpt)(Gly-Gly)]ClO$_4\cdot$H$_2$O in polyethylene pellet at 6 K is represented in Figure 4. It exhibits two main bands, one at 21035 cm^{-1} (ν_1) and the other at 27670 cm^{-1} (ν_2) corresponding to the $^4A_{2g} \rightarrow ^4T_{2g}$ and $^4A_{2g} \rightarrow ^4T_{1g}$ (O_h) transitions, respectively. The low temperature spectrum exhibits some interesting broad band splittings. The resolved spectrum was obtained using Gaussian function. Good fit to spectrum was possible with six peaks under spectrum, that is, three Gaussian curves for each observed band, and this can be seen in Figure 4. The band of highest energy is due to background correction. A deconvolution procedure on the experimental band pattern yielded maxima at 19760, 21720, 24330, 25220, 27410 and 28090 cm^{-1} for the noncubic splittings of $^4T_{2g}$ and $^4T_{1g}$.
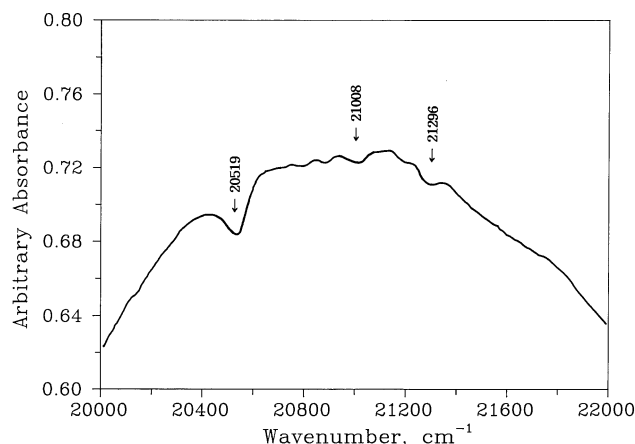
Due to the low symmetry of the complex both quartet states split into three components. Considering C_{2v} symmetry we obtain the following states:

$$^4A_2 (^4A_{2g}) << ^4A_1, ^4B_1, ^4B_2 (^4T_{2g}) < ^4A_2, ^4B_1, ^4B_2 (^4T_{1g})$$

Static selection rules predict the transition into $^4A_1$ to be the only not electric- dipole allowed. This would fit the small intensity but not the sharpness of the third band, which looks more like a doublet mixed with a quartet of the same symmetry. The ligand field calculations shows, however, no doublets in this spectral region. All transitions become allowed by dynamic selection rules. So it is hard to decide if there is the third transition hidden under the intense second band. In the $^4T_{1g}$ region it is reasonable to deal with three bands obtained by the fit procedure, although band maxima can not be determined in high precision. Then these deconvoluted bands were included for ligand field parameterization. There are very small features in the shape around the maximum of the first quartet band. To us it looks like an
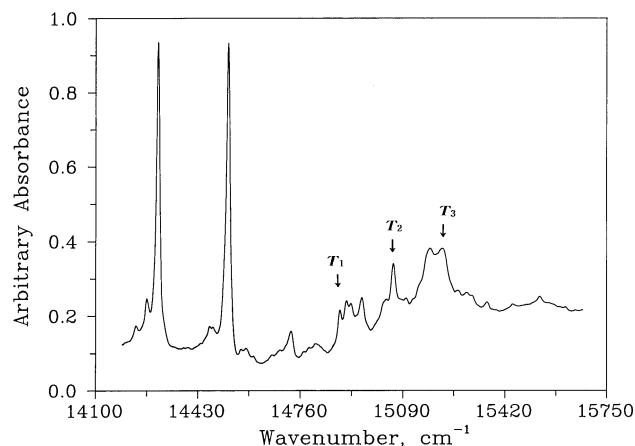

Figure 5. Expanded portion of the absorption spectrum showing $^4A_{2g} \rightarrow ^2T_{2g}$ electronic origins.

antiresonance effect due to the close-lying states $^2T_{2g}$ and $^4T_{2g}$, which allows for the location of the lowest component of $^2T_{2g}$ as shown Figure 5.

The sharp-line absorption spectrum of *mer*-[Cr(dpt)(Gly-Gly)]ClO$_4\cdot$H$_2$O measured as microcrystalline powders in a polyethylene matrix at 2 K is shown in Figure 6. The ^2E_g (O_h) origins, which are separated by 211 cm^{-1}, are located with two very strong peaks at 14294 and 14505 cm^{-1} in the low energy side of the absorption spectrum. They are easily assigned to the two components (R_1 and R_2) of the $^4A_{2g} \rightarrow ^2E_g$ transition. The lowest-energy zero-phonon line coincides within 9 cm^{-1} with the emission origin. The 211 cm^{-1} splitting is larger than the 145 cm^{-1} and 158 cm^{-1} observed for K[Cr(Gly-Gly)$_2$] and [Cr(ida)(dpt)]ClO$_4\cdot$2H$_2$O complexes, respectively.[5,6]

A relatively intense peak at 540 cm^{-1} from the lowest electronic line, R_1, can be assigned as a first component, T_1 of the $^2T_{1g}$ group because it has no correspondence in the emission and infrared spectra. As expected, a difficulty was experienced in the assignment of two remaining electronic origins because the intense vibronic structure of ^2E_g covers most of the arising from the $^4A_{2g} \rightarrow ^2T_{1g}$ transition. In gen-

Figure 4. Resolved visible absorption spectrum of *mer*-[Cr(dpt)(Gly-Gly)]ClO$_4\cdot$H$_2$O at 6 K.

Figure 6. The sharp-line absorption spectrum of *mer*-[Cr(dpt)(Gly-Gly)]ClO$_4\cdot$H$_2$O measured as microcrystalline powders in a polyethylene matrix at 2 K.

Absorption and IR Spectra of [Cr(dpt)(Gly-Gly)]ClO₄

Bull. Korean Chem. Soc. **1999**, Vol. 20, No. 4   439

eral the electronic origins are more intense than the vibronic peaks in the same region. We assign relatively intense peaks at 699 and 845 cm^{-1} from the lowest electronic line, R_1 as two components, T_2 and T_3 because some higher peaks are related also to that origin as vibrational sidebands.

AOM Calculations. The ligand field analysis was carried out through an optimized fit of experimental to calculated transition energies. The doublet and quartet energies with the appropriate degeneracies are calculated by diagonalizing the full 120×120 secular matrix which arises from the perturbed d^3 system.[24] Eigenvalues were assigned to quartet or doublet states based on a spin analysis of the corresponding eigenfunctions. The amount of quartet character in the doublet states was estimated by comparing the eigenfunctions of the excited doublet states with and without spin-orbit coupling. The ligand field potential matrix was generated for *mer*-[Cr(dpt)(Gly-Gly)]ClO₄·H₂O from just the six atoms in the first coordination sphere with the exact ligand positions obtained from the X-ray crystal structure.[4] The coordinates were then rotated so as to maximize the projections of the six-coordinated atoms on the Cartesian axes centered on the chromium. The resulting optimized Cartesian and spherical polar coordinate for ligating atoms and adjacent carbons are listed in Table 2. Although the perchlorate oxygens may also perturb the metal d orbitals, the extent of that interaction was judged too small to warrent any additional adjustable parameters.

The π-interactions of the carboxylate oxygen and peptide nitrogen with the metal ion were considered to be anisotropic. The π bonding was described by parallel and perpendicular contributions with respect to the orientation of the π systems of the ligands. For the anistropic ligands of the parameter ratio $e_{\pi c}/e_{\pi s}$ was chosen to 0.6 from reasonable values of the corresponding overlap integrals.[25] Since the π interaction of amine nitrogens with sp^3 hybridization was assumed to be negligible, the eight parameters are involved in the ligand field optimizations. The AOM parameters $e_{\sigma Np}$ and $e_{\pi Np}$ for the peptide nitrogen-chromium, $e_{\sigma O}$ and $e_{\pi O}$ for the carboxylate-chromium interaction, and $e_{\sigma N}$ for the amine-chromium interaction, interelectronic repulsion parameters and the Trees[26] correction parameter α_T are required to fit fifteen experimental energies: the five $^4A_{2g} \rightarrow \{^2E_g, ^2T_{1g}\}$ components, identified in Table 3, the three $^4A_{2g} \rightarrow ^2T_{2g}$ components, the six $^4A_{2g} \rightarrow \{^4T_{2g}, ^4T_{1g}\}$ components,

and the splitting of the ^2E_g state. We have varied each parameter in order to find its characteristic influence on the energy level scheme. Then we used the optimization routine for the final results. As expected, the Racah parameters do actually not influence the low-symmetry level splittings considered here. In order to reduce the parameter space to a minimum, we could use parameter values which can be obtained in first good approximation from the quartet band separation ($^4T_{1g}$ - $^4T_{2g} \approx 12B$) and from the energy position of lowest doublet term (^2E_g - $^4A_{2g} \approx 9B + 3C$). Since the AOM parameters have been found to be transferable between similar compounds, $e_{\sigma N}$ for the amine nitrogen has been well established from calculations on other chromium(III) complexes[10,12,27] to have a value around 7200 cm^{-1}. We found that the influence of increasing zeta on the doublet pattern was relatively small. Therefore, the spin-orbit coupling parameter ζ is set at 200 cm^{-1}. Racah parameters depend on the value of Trees parameter which is included in the calculations. It is also fixed at 125 cm^{-1}. Finally, we tried to improve the calculated energy level scheme by using a fitting procedure which is based on the Powell parallel subspace algorithm.[28] We started with the optimization of e_σ and e_π values of the O and N$_p$ ligator atoms, other parameters being assigned to reasonable values (see above). In a second step, all parameters involved except ζ and α_T were allowed to vary freely. The results of the optimization and the parameter set used to generate the best-fit energies are listed in Table 3. The quartet terms were given a very low weight to reflect the very large uncertainty in their position.[29]

The AOM results are plausible and reproduce the spectrum pretty well. The following values were finally obtained for the ligand field parameters: $e_{\sigma O} = 8965 \pm 110$, $e_{\pi O} = 1892 \pm 20$, $e_{\sigma Np} = 7702 \pm 80$, $e_{\pi Np} = 477 \pm 50$, $e_{\sigma N} = 7022 \pm 80$,

Table 3. Experimental and calculated electronic transition energies for *mer*-[Cr(dpt)(Gly-Gly)]ClO₄·H₂O^a

State (O_h)	Exptl	Calcd^b
^2E_g	14294	14312
	14505	14499
$^2T_{1g}$	14834	14546
	14993	14744
	15139	15050
$^2T_{2g}$	20519	21528
	21008	21999
	21296	22334
$^4T_{2g}$	19760	19504
	21720	20913
	24330	21148
$^4T_{1g}$	25220	25395
	27410	27233
	28090	28383

^{a} Data in cm^{-1}. ^{b} $e_{\sigma O} = 8965 \pm 110$, $e_{\pi O} = 1892 \pm 20$, $e_{\sigma Np} = 7702 \pm 80$, $e_{\pi Np} = 477 \pm 50$, $e_{\sigma N} = 7022 \pm 80$, $B = 690 \pm 6$, $C = 2838 \pm 15$, $\alpha_T = 125$ (fixed), $\zeta = 200$ (fixed).

Table 2. Optimized Cartesian and spherical polar coordinates for ligating and adjacent atoms in *mer*-[Cr(dpt)(Gly-Gly)]$^{+ a}$

Atom	x	y	z	θ	ϕ	ψ
N$_p$	0.002	-1.904	0.053	88.40	- 89.93	-7.14
O$_c$	-0.013	-0.242	-1.926	172.82	-93.14	4.37
N$_a$	0.022	-0.260	2.103	7.07	-85.21	
N$_1$	2.097	0.018	0.074	87.99	0.48	
N$_2$	0.053	2.195	0.010	89.74	88.63	
N$_3$	-2.084	-0.036	0.040	88.91	-179.02	
C$_1$(N$_p$)	0.141	-2.562	1.172			
C$_2$(O$_c$)	0.170	-1.466	-2.336			

^{a} Cartesian coordinates in Å, polar coordinates in degrees.

$B = 690\pm6$, $C = 2838\pm15$ cm^{-1}. The $e_{\sigma N}$ value for amine nitrogen is located in the normal range. The results for carboxylate oxygen confirm the characterization of the this ligand as a strong σ- and a strong π-donor. The value of 7702 cm^{-1} for the $e_{\sigma Np}$ is comparable to values for other amines.[19] The positive value of 477 cm^{-1} for $e_{\pi Np}$ corresponds to less π-donating ability than carboxylate group. We also can see that the ligand field theory reproduce experimentally observed large splitting of 211 cm^{-1} of ^2E_g (O_h) state. An orbital population analysis yields a configuration of $(xy)^{1.009}(xz)^{0.947}(yz)^{1.027}(x^2\text{-}y^2)^{0.011}(z^2)^{0.016}$ for the lowest component of ^2E_g state. The relative d-orbital ordering from the calculation is that $E(xy) = 475$ cm$^{-1} < E(xz) = 712$ cm$^{-1} < E(yz) = 1953$ cm$^{-1} < E(x^2\text{-}y^2) = 21530$ cm$^{-1} < E(z^2) = 22456$ cm^{-1}. These factors plus AOM parameters can be used for predicting the photolabilization modes and interpreting the photostereochemistry of the chromium(III) complexes.[30] The value of Racah parameter, B is about 75% of the value for a free chromium(III) ion in the gas phase. Since dipeptides are present in biological systems further research ought to be directed towards the possible role of such compounds in biological processes. Meridional coordination at active sites may be possible in reactions catalyzed by metalloenzymes.

References

1. Murdoch, C. M.; Cooper, M. K.; Hambley, T. W.; Hunter, W. N.; Freeman, H. C. *J. Chem. Soc., Chem. Comm.* **1986**, 1329.
2. Subramaniam, V.; Lee, K. W.; Garvey, R. G.; Hoggard, P. E. *Polyhedron* **1988**, *7*, 523.
3. Choi, J. H.; Hoggard, P. E. *Polyhedron* **1992**, *11*, 2399.
4. Choi, J. H.; Suh, I. H.; Kwak, S. H. *Acta Cryst.* **1995**, *C51*, 1745.
5. Subramaniam, V. *Ph. D. Thesis*; North Dakota State University: 1989.
6. Subramaniam, V.; Lee, K. W.; Hoggard, P. E. *Inorg. Chim. Acta* **1994**, *216*, 155.
7. Schönherr, T. *Inorg. Chem.* **1986**, *25*, 171.
8. Schmidtke, H. H.; Adamsky, H.; Schönherr, T. *Bull. Chem. Soc. Jpn.* **1988**, *61*, 59.
9. Hoggard, P. E. *Top. Curr. Chem.* **1994**, *171*, 114.
10. Schönherr, T.; Wiskemann, R.; Mootz, D. *Inorg. Chim. Acta* **1994**, *221*, 93.
11. Schönherr, T. *Top. Curr. Chem.* **1997**, *191*, 87.
12. Schönherr, T.; Itoh, M.; Urushiyama, A. *Bull. Chem. Soc. Jpn.* **1995**, *68*, 2271.
13. Fujihara, T.; Schönherr, T.; Kaizaki, S. *Inorg. Chim. Acta* **1996**, *249*, 135.
14. Schönherr, T.; Atanasov, M.; Hauser, A. *Inorg. Chem.* **1996**, *35*, 2077.
15. (a) Choi, J. H. *J. Photosci.* **1996**, *3*, 43. (b) Choi, J. H. *J. Photosci.* **1997**, *4*, 127. (c) Choi, J. H.; Oh, I. G. *Bull. Korean Chem. Soc.* **1997**, *18*, 23.
16. (a) Choi, J. H. *Bull. Korean Chem. Soc.* **1997**, *18*, 819. (b) Choi, J. H. *Bull. Korean Chem. Soc.* **1998**, *19*, 575. (c) Choi, J. H. *Bull. Korean Chem. Soc.* **1999**, *20*, 81.
17. Hoggard, P. E. *Coord. Chem. Rev.* **1986**, *70*, 85.
18. Schönherr, T.; Spanier, J.; Schmidtke, H. H. *J. Phys. Chem.* **1989**, *93*, 5969.
19. Wermuth, M.; Riedener, T.; Güdel, H. U. *Phys. Rev.* **1998**, *57B*, 4369.
20. Gainsford, A. R.; Schmidtke, H. H. *Inorg. Chim. Acta* **1972**, *6*, 227.
21. Schmidtke, H. H.; Garthoff, D. *Inorg. Chim. Acta* **1968**, *2*, 357.
22. Subramaniam, V.; Hoggard, P. E. *Inorg. Chim. Acta* **1989**, *155*, 161.
23. (a) Choi, J. H. *Bull. Korean Chem. Soc.* **1993**, *14*, 118. (b) Choi, J. H.; Oh, I. G. *Bull. Korean Chem. Soc.* **1993**, *14*, 348. (c) Choi, J. H. *Bull. Korean Chem. Soc.* **1994**, *15*, 145.
24. Smith, B. T.; Boyle, J. M.; Dongarra, J. J.; Garbow, B. S.; Ikebe, Y.; Klema, V. C.; Moler, C. B. *Matrix Eigensystem Routines-EISPACK Guide*; Spring-Verlag: Berlin, 1976.
25. Schönherr, T.; Degen, J. *Z. Naturforsch.* **1990**, *45A*, 161.
26. Trees, R. E. *Phys. Rev.* **1951**, *83*, 756.
27. Schönherr, T.; Schmidtke, H. H. *Inorg. Chem.* **1979**, *18*, 2726.
28. Kuester, J. L.; Mize, J. H. *Optimization Techniques with Fortran*; McGraw-Hill: New York, 1973.
29. Clifford, A. A. *Multivariate Error Analysis*; Wiley-Hasted: New York, 1973.
30. Vanquickenborne, L. G.; Ceulemans, A. *Coord. Chem. Rev.* **1983**, *48*, 157.